Peer-reviewed version available at *Materials* **2018**, *11*, 1147; doi:10.3390/ma11071147

Article

Mechanical Properties and Carbonation Durability of Engineered Cementitious Composites Reinforced by Polypropylene and Hydrophilic Polyvinyl Alcohol Fibers

Wei Zhang [1], Chenglong Yin [1], Fuquan Ma [1], and Zhiyi Huang [1,*]

[1] College of Civil Engineering and Architecture, Zhejiang University, 866 Yuhangtang Road, Hangzhou Zhejiang Province, 310000, China; zhangw8778@zju.edu.cn; yinchenglong@zju.edu.cn; mafuquan@zju.edu.cn

* Correspondence: hzy@zju.edu.cn; Tel.: +86-0571-88208702

Abstract: Herein, the mechanical properties and carbonation durability of engineered cementitious composites (ECC) were studied. For cost-efficient utilization of ECC materials, polypropylene (PP) and hydrophilic polyvinyl alcohol (PVA) fibers were employed to cast different types of specimens. The compressive strength, Poisson's ratio, strength-deflection curves, cracking/post-cracking strength, impact index, and tensile strain-stress curves of the two types of ECC materials, with different fiber contents of 0 vol%, 1 vol%, 1.5 vol% and 2 vol%, were investigated by conducting compressive tests, four-point bending tests, drop weight tests, and uniaxial tensile tests. In addition, the matrix microstructure and failure morphology of the fiber in the ECC materials were studied by scanning electron microscopy (SEM) analysis. Furthermore, carbonation test and steel corrosion after carbonization were employed to study durability resistance. The results indicated that for both PP fiber- and hydrophilic PVA fiber-reinforced ECCs, the compressive strength first increases and then decreases as fiber content increases from 0 vol% to 2 vol% and reaches the maximum at 1 vol% fiber content. The bending strength, deformation capacity, and impact resistance show significant improvement with increasing fiber contents. The ECC material reinforced with 2 vol% PP fiber shows superior carbonized durability with maximum carbonation depth of only 0.8 mm.

Keywords: cost-efficiency; SHCC; ECC; PP fiber; hydrophilic PVA fiber; carbonation durability

1. Introduction

The inherent quasi-brittleness of conventional cementitious materials produces lower strain capacity and damage tolerance, leading to poor safety and low durability for infrastructures like building, bridges, tunnels, etc. In recent years, a strain hardening cementitious composite (SHCC) containing high volume of polymer fibers (up to 2 vol% fraction) has been shown to exhibit a pseudo strain-hardening ability under direct tensile stress and has been investigated and utilized for many applications [1-3]. Compared with ordinary concrete, the main advantages of SHCC materials are the much higher ductility and deformation capacity after initial cracking; therefore, SHCC materials show higher load-carrying ability, thus enhancing safety and durability for structures under catastrophic conditions [4-5].

ECC is the most typical type of SHCCs, which was first reported by Li. in 1994 [6-7]. The main theory for the design of ECC involves a cohesive crack-mechanics approach with two nondimensionalized parameters from steady-state cracking and multiple cracking (Li and Leung, in 1992) [8]. ECC is well known for its strain-hardening ability and fine multi-cracking failure mode under uniaxial tension load and its tensile strain capacity can reach 3–5%, whereas the ultimate crack width is restricted to only 60–100 μm [9-10]. Recently, a new kind of ECC material with tensile strain capacity as large as 8% has been manufactured with randomly dispersed polyethylene (PE) fiber [11].

Therefore, the use of ECC could significantly improve the durability [12-13] of concrete components and structures, thereby reducing maintenance cost during their lifetime and meeting the demands of modern civil engineering.

The relatively high strain capacity and multiple cracking abilities of the ECC materials are significantly dependent on the fiber geometry, aspect ratio, volume fraction, etc. of the fibers [14-15] In light of early developments, the two most commonly used polymer fibers in ECC materials are polyethylene (PE) and oiled polyvinyl alcohol fibers (PVA, manufactured by manufactured by Kuraray CO., LTD, in Japan) [16-17]. However, the costs per unit volume of PE and PVA fiber are ten or more times higher than that of ordinary concrete, which increases the cost of manufacturing and limits the practical engineering applications of ECC. Thus, it is worthwhile to develop cost-effective fiber-reinforced ECC materials [18]. One way to achieve this is the use of hybrid fibers as toughening components. Zhang, et al. [19-20] investigated the mechanical properties of ECC reinforced by PVA-steel hybrid fiber, and have showed that the individual crack width decreases significantly during the multi-cracking stage, but the cracking and tensile strength increase with increasing steel fiber content. Hamid [10, 21] studied the improvement in ductility of PVA-PP hybrid fiber-reinforced ECC, and the results indicated that both the flexural strength and ductility of the composites were higher than the non-reinforced material. The other solution is the use of cost-efficient PP fiber and hydrophilic PVA fiber in the matrix. Huang et al [18] investigated the performance of PP-ECC beams under reversed cyclic loading, and showed that energy dissipation capacity of the PP-ECC beam is 2.9-times higher than that of ordinary concrete, and that less damage appeared in the PP-ECC beam due to the load carrying capacity of the PP fiber in the cement matrix. Sasma [22] and Pan [13] considered the strong chemical bond between the fiber and the matrix and found that due to the hydrophilicity of the unoiled PVA fiber, rupture during multi-cracking stage was the limiting factor of strain capacity instead of pull-out failure. Furthermore, increment in fiber content could increase flexural strength, bending ductility, and toughness.

The composition of ECC matrix is quite different from that of conventional concrete. According to micromechanical analysis, elimination of coarse aggregates produces high cement content (2–3 times higher than that in ordinary concrete), and large quantities of fine sand used in the matrix also increases the cost of ECC. Therefore, replacement of cement with fly ash and increasing use of local ingredients are adopted for ECC design [23-24].

In view of this, this study is concerned with the practical use of ECC materials, and the main objective is to study the effects of low-cost fibers (PP fiber and hydrophilic PVA fiber) and relativity coarse sand (maximum particle size of 0.6 mm) employed in ECC materials.

2. Materials and Methods

2.1. Material properties

The use of local ingredients plays a major role in reducing cost and improving practical engineering applications of ECC [16, 23]. Matrix materials employed herein included Portland cement (PC), fly ash (FA), silica sand, expansive agent, and polycarboxylate superplasticizer (PSP). Type-Ⅱ 52.5-R Portland cement, manufactured by Conch Cement Co., Ltd, China, has a specific surface area of 365.3 m^2/kg, an initial setting time of 123 min, and a final setting time of 181 min. Fly ash employed in this study is Class-F with low calcium content. The chemical compositions of both PC and FA are shown in Table 1. The particle size of silica sand ranges from 0 to 0.6 mm. Considering the latent higher shrinkage during hydration [25-27], an expansion agent mixed in matrix is necessary. Calcium sulfoaluminate (CSA), the expansion agent used herein, is manufactured by Tianjin BaoMing Co., Ltd, China. PSP is used to improve the flowability of the mixture.

Two types of fibers were employed in this study: chopped polypropylene fibers (PP fiber) and hydrophilic polyvinyl alcohol fiber (HPVA fiber), supplied by Tianyi Company and BHL Company from China, respectively. The physical properties of the PP and HPVA fibers are given in Table 2, and the SEM images are given in Figure 1.

Table 1. Chemical compositions of PC and FA.

Materials	Chemical compositions (mass fraction, %)

Preprints (www.preprints.org) | NOT PEER-REVIEWED | Posted: 7 June 2018 doi:10.20944/preprints201806.0126.v1

Peer-reviewed version available at Materials 2018, 11, 1147; doi:10.3390/ma11071147

	SiO_2	Al_2O_3	Fe_2O_3	CaO	MgO	SO_3	NaO	K_2O
PC	9.68	3.63	3.91	50.59	1.55	1.45	0.12	0.39
FA	26.44	15.2	7.11	9.07	1.3	0.83	0.95	1.57

Table 2. Physical properties of PP fiber and HPVA fiber.

Name	Diameter (mm)	Tensile strength (MPa)	Tensile modulus (GPa)	Length (mm)	Density (g/cm3)	Elongation percentage (%)
PP	16	≥500	3.5	12	0.91	15~20
HPVA	39	≥1600	42.8	12	1.3	6~8

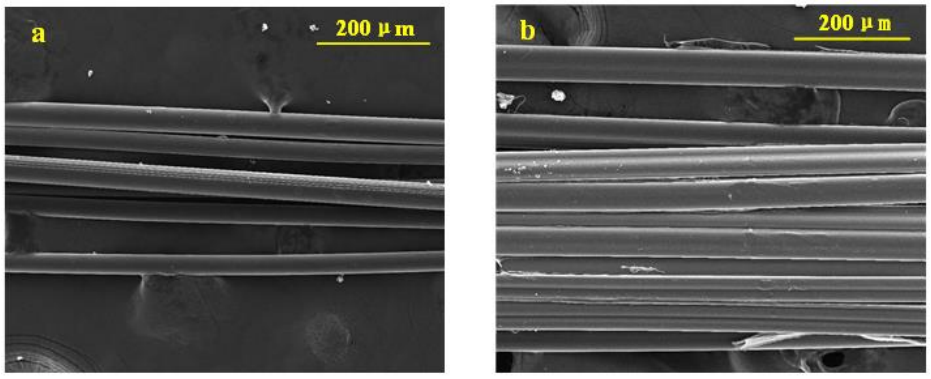

Figure 1. SEM photos: (a) PP fiber; and (b) HPVA fiber.

Table 3. Mix properties of PCC, PP-ECC and HPVA-ECC.

Groups	Volume Fraction (%)		Weight Ratio of Matrix					
	PP	PVA	PC	FA	Water	Silica Sand	CSA	PSP
PCC	0	0						
PP-ECC-1%	1	0						
PP-ECC-1.5%	1.5	0						
PP-ECC-2%	2	0	1	0.9	0.6	0.8	0.1	0.1%
HPVA-ECC-1%	0	1						
HPVA-ECC-1.5%	0	1.5						
HPVA-ECC-2%	0	2						

2.2. Mix design

In the current study, seven types of mixtures were casted, the composition details of which are listed in Table 3. Calculated amounts of CSA were added to the binders. Water-to-binder ratio was 0.3, silica sand-to-binder ratio was 0.4, and PSP occupied 0.2 wt% of total binders. The proportion of matrix was the same in all the samples. Fiber contents of 1 vol%, 1.5 vol%, and 2 vol% of both PP fiber and hydrophilic PVA fiber were used and a plain cementitious composite (PCC) was prepared as a reference. All the mixtures were demolded after 24 h at room temperature and were cured for up to 28 days at a temperature of 23℃±2℃ and under relative humidity of 95%±5%.

2.3. Experimental work

The experimental program is divided into mechanical property tests and durability test. In the first part, the effects of the types and contents of fiber on compressive behavior, four-point bending performance, and drop weight test were studied, and the typical tensile behavior of ECC with 2 vol% fiber is analyzed. In the durability test, the carbonation resistance of 2 vol% PP-fiber-reinforced ECC (PP-ECC) and the corrosion depth of rebar caused by carbonation are studied.

Mechanical property tests: The compressive tests of PP-ECC and hydrophilic PVA-ECC materials were performed by testing cylinder-shaped specimens of dimensions Φ150 mm × 300 mm. Each group contained 3 samples, and a total of 21 cylinders were casted. All the cylinders were loaded

Preprints (www.preprints.org) | NOT PEER-REVIEWED | Posted: 7 June 2018 doi:10.20944/preprints201806.0126.v1

Peer-reviewed version available at Materials 2018, 11, 1147; doi:10.3390/ma11071147

into a 200t pressure tester. Considering the errors caused by uneven surface during casting, preloading was done with a rapid-hardening plaster in the cast surface to ensure flat surfaces. The deformation curve was measured by two symmetrically arranged extensometers. A uniaxial load was applied at a rate of 0.5–0.8 MPa/s. Two vertical and two horizontal strain gauges were glued at mid-height of each samples for measuring the Poisson's ratio.

Prismatic beams with dimensions of 100 mm × 100 mm × 400 mm were employed for the testing the four-point bending (4PB) performance. For measuring the mid-span deflections, a steel strip was fixed on the cross beams at the top position with a hot melt adhesive as a measuring point. The deflection values in the displacement control mode at a rate of 0.1 mm/min was measured by two symmetrically arranged linear variable differential transformers (LVDTs). The details of the 4PB tests are shown in Figure 2.

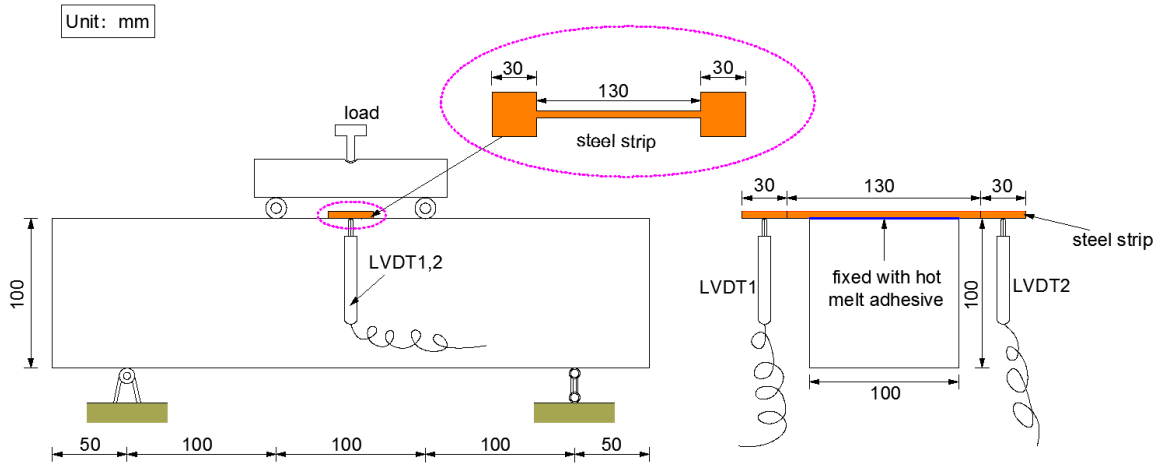

Figure 2. Details of 4PB tests.

Impact resistance behavior was studied by the drop weight test (ACI 544.2R-1999), dimension of samples being Φ150 mm × 63 mm. Each specimen was impacted by a 4.5-kg drop hammer dropped from a height of 0.5 m to produce impact energy.

Sheet-shaped specimens of dimensions 15 mm × 50 mm × 350 mm were subjected to uniaxial tensile test [13]. Considering the end damage caused by stress concentration, carbon fiber cloth and aluminum plate were used to strengthen the ends of the specimens with a length of 100 mm. The deflection of uniaxial tensile tests was measured by two symmetrically arranged LVDTs in deflection control model at a rate of 0.1 mm/min.

Durability test: The samples used in the carbonization test were beams of dimensions 100 mm × 100 mm × 400 mm. After curing for 28 d under standard conditions, five surfaces of each sample were sealed with paraffin and only one longitudinal surface was left untreated. When the carbonation test was outperformed, the concentration of CO_2 gas in the carbonization chamber was controlled at 20 ± 3%. After erosion for 3 d, 7 d, 14 d, and 28 d, respectively, a 50-mm-long section was cut off from one end of each sample and the new face of the rest part was immediately waxed. Strike lines were drawn on the cut-off specimen every 10 mm and sprayed with 1% phenolphthalein alcohol solution (PAS) to measure the depth of carbonation based on the color change of PAS. The details of the carbonation test are shown in Figure 3.

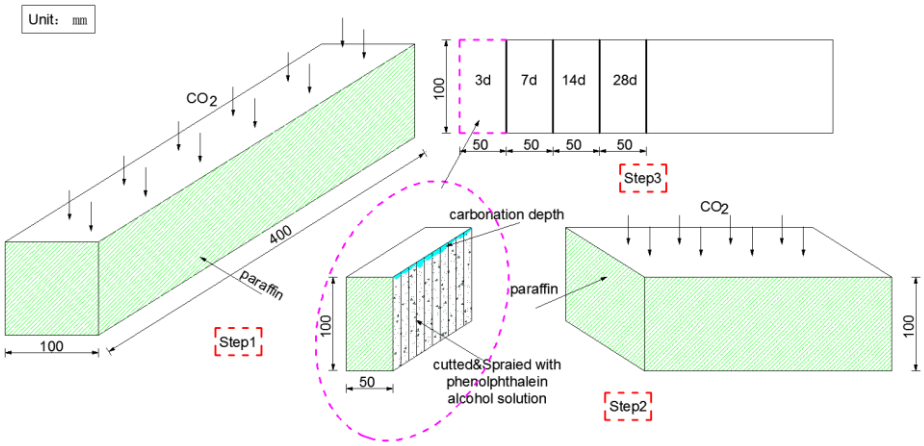

Figure 3. Details of carbonization test.

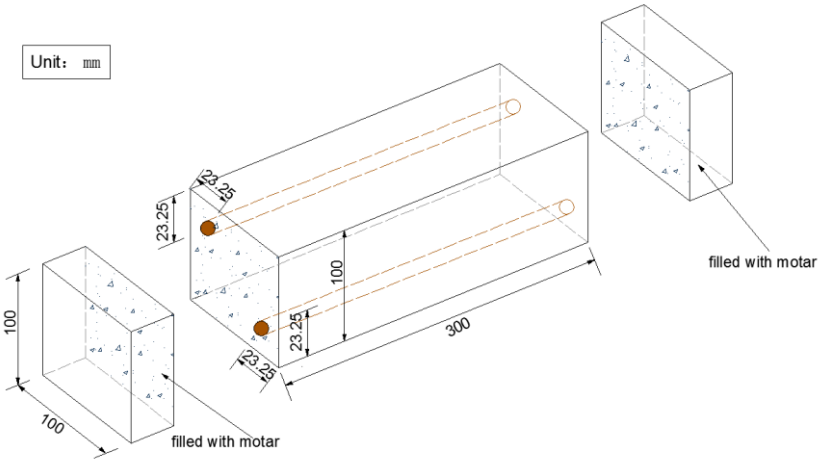

Figure 4. Details of the rebar corrosion test after carbonation.

Considering the corrosion of rebar due to the carbonization of concrete cover, which reduces the durability for the structures, reinforcement corrosion after carbonation was investigated. Two rebars of diameter 6.5 mm and length 300 mm were embedded in the PP-ECC (2% volume of PP fiber). After a curing period of 28 d under standard conditions, the specimens were put in the carbonization chamber for another 28 d to simulate a 50-year corrosion process under ordinary conditions. After this, all the samples should be cured under standard conditions for 28 more d. Results of this test were obtained by measuring the weight loss of rebars. Considering the weight loss caused by acid wash, two plain rebars were employed to modify this condition. Details of the reinforcement corrosion under carbonation are shown in Figure 4.

3. Result and discussion

3.1. Mechanical property test

Compressive test: The compressive strength and Poisson's ratio are reported as averages of the values obtained for three samples in each group. The relations of compressive strength and Poisson's ratio with the types and volume fractions of fibers are given in Figures 5 (a) and (b), respectively. Error bar indicates the location of average value between the maximum and minimum values.

Preprints (www.preprints.org) | NOT PEER-REVIEWED | Posted: 7 June 2018 doi:10.20944/preprints201806.0126.v1

Peer-reviewed version available at Materials 2018, 11, 1147; doi:10.3390/ma11071147

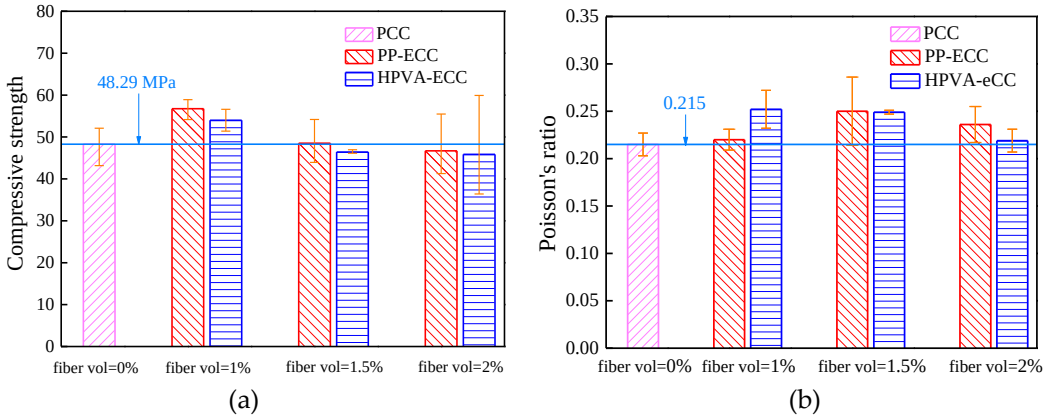

Figure 5. Results of compressive test: (a) Compressive strength, and (b) Poisson's ratio.

As shown in Figure 5(a), the compressive strength of PCC is 48.29 MPa. After mixing with PP and HPVA fibers, compressive strength increases up to a fiber content of 1 vol% and declines gradually for fiber contents greater than 1 vol%. This may be because randomly distributed fibers could strengthen the matrix and control cracking propagation, thereby enhancing compressive strength [28]. However, when the fiber content exceeded 1 vol%, the high volume fraction of fibers could not disperse evenly in the matrix, producing more air bubbles and thus reducing compressive strength [29]. Compared to the PCC, specimens with 1 vol% PP fiber and hydrophilic PVA fiber showed 17.5% and 6.44% enhancement in compressive strength, respectively, whereas the compressive strengths of those with 2 vol% fiber content decrease by ~3.3% and 14.6%, respectively. These results are similar to those reported by Pan's group [30]. Moreover, fibers can control sliding and extending of micro-cracks, which limits lateral expansion and enhances Poisson's ratio compared with PCC (Figure 5(b)).

Furthermore, as can be seen in Figure 5, all the specimens mixed with PP fiber have higher compressive strength than the HPVA fiber-reinforced ones for the same fiber content. In general, composites with high-modulus fiber exhibit higher strength [20, 29, 31]. In this study, although the modulus of HPVA fiber (42.8 GPa) is much higher than that of PP fiber (3.5 GPa), opposite results are obtained because of the poor dispersivity of the HPVA fiber.

4PB test: The strength-deflection curves for all the 4PB tests (Figure 6) show that all the specimens possess dramatically high ductility and load-deflection hardening ability under the 4PB test conditions. The shape of the load-deflection curves were highly influenced by the fiber types and contents, which is essential for choosing appropriate ECCs in bending structures of different requirements. The area enclosed by load-deflection curve increases with increasing fiber contents, indicating that higher fiber fraction yields higher energy absorption capacity [21].

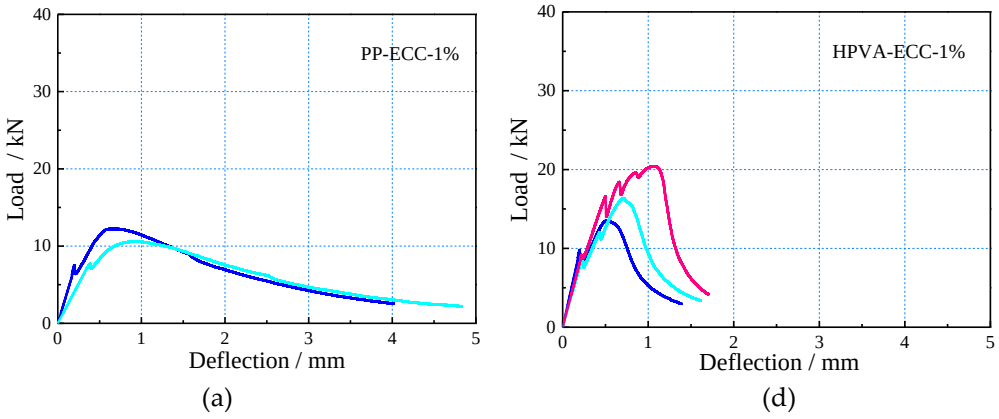

Preprints (www.preprints.org) | NOT PEER-REVIEWED | Posted: 7 June 2018 doi:10.20944/preprints201806.0126.v1

Peer-reviewed version available at Materials 2018, 11, 1147; doi:10.3390/ma11071147

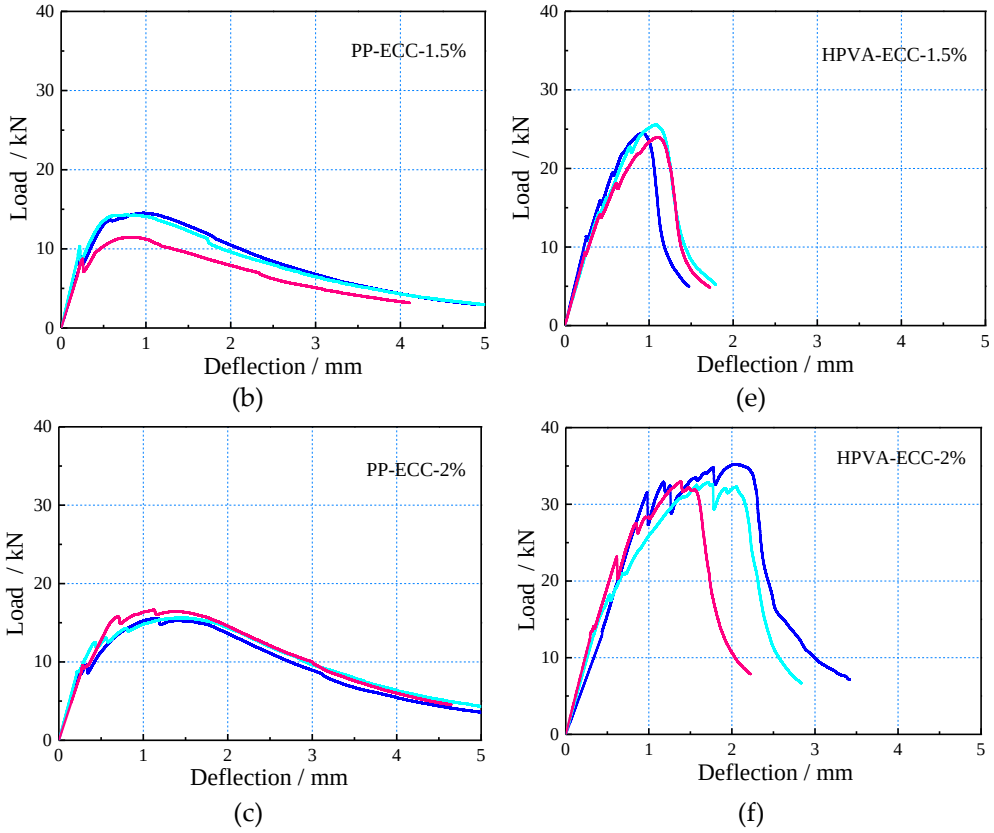

Figure 6. Load-deflection curves: (a) PP-ECC-1%, (b) PP-ECC-1.5%, (c) PP-ECC-2%, (d) HPVA-ECC-1%, (e) HPVA-ECC-1.5%, and (f) HPVA-ECC-2%.

Cracking and post-cracking strength also increased with increasing fiber contents (Figure 7). Composites reinforced with PP fiber show higher deformability but lower strength than those with hydrophilic PVA fibers for the same fiber content, which may be because PP fibers have lower elastic modulus and tensile strength than HPVA fibers. Furthermore, by comparing the load-deflection curves of the two kinds of ECCs with the same fiber contents, it can be found that specimens containing PP fibers show less softening response after post-cracking than those containing HPVA fibers.

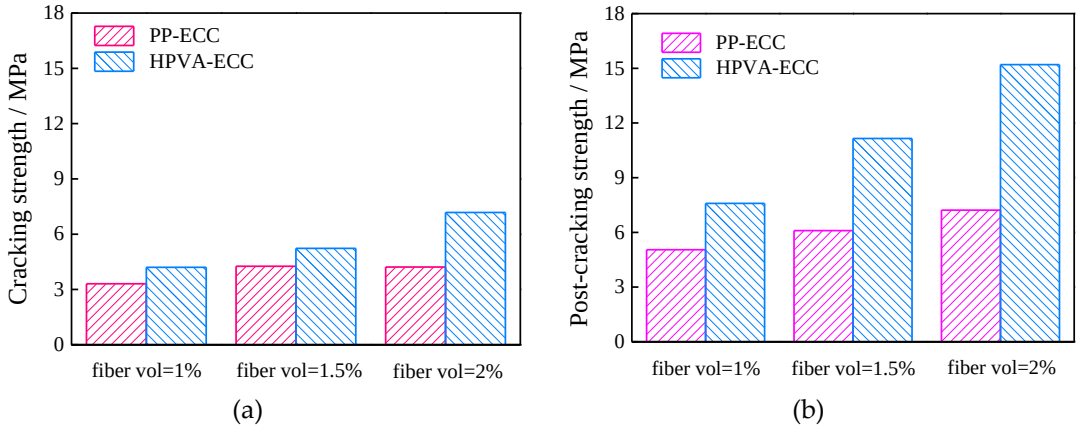

Figure 7. Results for (a) Cracking strength, and (b) Post-cracking strength.

There are pronounced three stages in a typical load-deflection curve: elastic stage, strain harden stage, and strain-softening stage (Figure 8).

Preprints (www.preprints.org) | NOT PEER-REVIEWED | Posted: 7 June 2018 doi:10.20944/preprints201806.0126.v1

Peer-reviewed version available at Materials 2018, 11, 1147; doi:10.3390/ma11071147

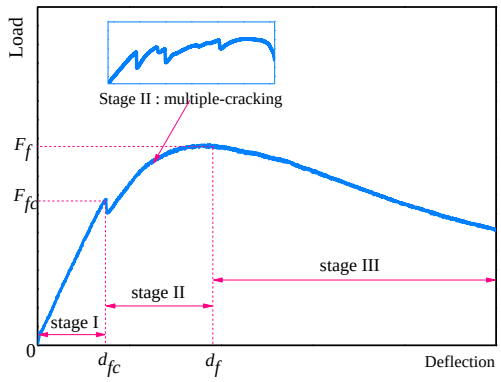

Figure 8. Typical bending load-deflection curves for ECC materials.

Based on Zhang's research[20], we can define bending property as follows. During stage I, the relationship between load and deflection is linear elastic until the first crack appears (F_{fc}, and d_{fc} are the corresponding stress and deflection). For ECC materials with 2 vol% of PP fiber and 1-2 vol% of hydrophilic PVA fiber, stage II represents the load-deflection hardening characteristics accompanied by the multiple-cracking phenomenon, and the post-cracking strength and the corresponding deflection are defined as F_f and d_f , respectively. During stage III, a main crack is localized and the load starts to decrease gradually.

Impact resistance test: The impact times needed to produce the first crack (N_1) and total failure (N_2) as well as the corresponding impact energies (W_1 and W_2) for specimens cured for 28 d are summarized in Table 4. The impact energy is determined by Eq (1). In addition, the typical failure forms of PP fiber- and PVA fiber-reinforced ECC with fiber fractions of 1 vol%, 1.5 vol%, and 2 vol% are shown in Figure 9.

$$W_i=N_i mgh \quad (1)$$

where m is the weight of the drop hammer (4.5 kg), g is the gravitational acceleration (9.81 m/s^2), and h is the drop height (0.5 m). Each group should remove the maximum and minimum values and adopt the average of the rest four values as the final values of N_1 and N_2.

Table 4. Impact resistance performance of PCC, PP-ECC and HPVA-ECC

Group	N_1(times)	W_1(J)	N_2(times)	W_2(J)
PCC	8	176.58	13.75	303.5
PP-ECC-1%	28.8	635.69	184.25	4066.86
PP-ECC-1.5%	29.5	651.14	428.5	9458.07
PP-ECC-2%	31	684.25	552.75	12200.57
HPVA-ECC-1%	146	3222.59	339.75	7499.13
HPVA-ECC-1.5%	411	9071.8	1212	26751.87
HPVA-ECC-2%	1285.5	283374.2	2664.5	58812.18

As can be seen in Table 4 and Figure 9, PCC without any fiber cracked after 8 hits and split into two or three fragments after 13.75 hits only. The corresponding impact energies were only 176.58 J and 303.5 J, respectively. The failure pattern shows overt brittle behavior. Conversely, after mixing with fiber to reinforce the cementitious composites, all the groups of ECC specimens exhibited higher impact toughness than PCC. The impact times for first crack and failure increased significantly with increasing fiber contents. For instance, when the PP fiber content increased from 1 vol% to 2 vol%, the impact times needed for crack and failure increased 3.6−3.9 times and 13.4−40.2 times, respectively. On the other hand, as the PVA fiber content increased from 1 vol% to 2 vol%, the impact times increased 18.3−160.7 times for first crack and 24.7−193.8 times for total failure. In addition, the type of fiber showed significant influence on the impact resistance. ECC specimens mixed with hydrophilic PVA fiber have much higher impact resistance than PP fiber-reinforced ones for the same fiber volume fraction. For instance, upon addition of 1 vol%, 1.5 vol%, and 2 vol% of PVA fiber, the impact times for crack and failure increased ~5.1/1.8 times, 13.9/2.8 times, and 41.5/4.8 times, respectively, compared with specimens containing the same volume fractions of PP fiber.

Preprints (www.preprints.org) | NOT PEER-REVIEWED | Posted: 7 June 2018 doi:10.20944/preprints201806.0126.v1

Peer-reviewed version available at Materials 2018, 11, 1147; doi:10.3390/ma11071147

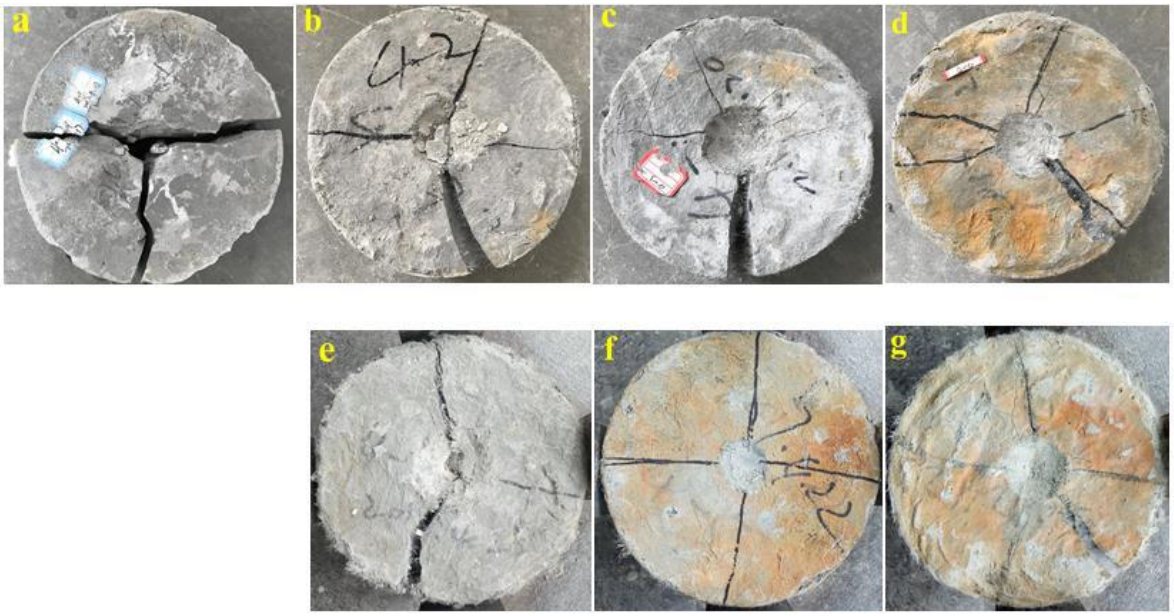

Figure 9. Typical fracture forms under drop weight test: (a) PCC, (b) PP-ECC-1%, (c) PP-ECC-1.5%, (d) PP-ECC-2%, (e) HPVA-ECC-1%, (f) HPVA-ECC-1.5%, and (g) HPVA-ECC-2%.

Figure 9 illustrates the typical impact failure form of specimens with different fiber types and contents. The failure mode of PCC shows apparent brittleness (Figure 9(a)). The first crack appears after an average of 8 hits and the main crack extends rapidly. Conversely, after mixing with PP and hydrophilic PVA fiber, ECC materials exhibit apparent ductility under impact loading. For instance, upon mixing with less than 1 vol% of fiber, the main crack of ECCs propagates slowly because of fiber bridging. The typical failure mode of PP-1% and PVA-1% specimens was three splitting fractures, as shown in Figures 9(b) and (e). Moreover, multi-crack was obtained by increasing fiber content, as shown in Figures 9(c), (d), (f) and (g). Based on these results, ECC materials mixed with hydrophilic PVA fiber showed higher impact resistances than those mixed with PP fiber.

Uniaxial tensile test result: The fracture mode of ordinary concrete under tensile stress is brittle failure and the tensile strain-stress curves are characterized by a linear elastic modulus up to failure. Therefore, ordinary concrete displays a sudden break-down failure mode without any warning. However, the main characteristic of ECC was strain-hardening after first cracking under tensile stress. Figure 10 illustrates the typical stress-strain curves of ECCs with 2 vol% PP fiber and 2 vol% hydrophilic PVA fiber after curing for 28 days.

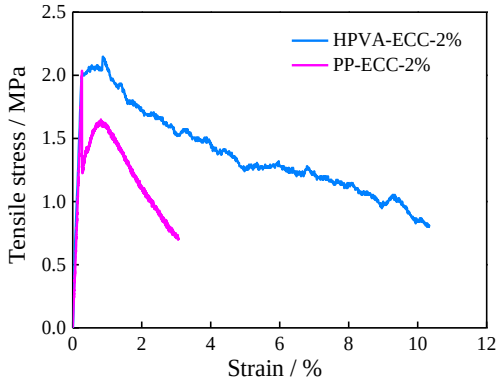

Figure 10. Tensile properties of PP-ECC and hydrophilic PVA-ECC.

Hydrophilicity of PVA fiber produces strong chemical bond with the matrix, which should be considered for strain-hardening and multi-cracking [9].However, the strain capacities of PP-ECC-2% and hydrophilic PVA-ECC-2% were 0.83% and 0.88%, 83-times and 88-times larger than ordinary

Preprints (www.preprints.org) | NOT PEER-REVIEWED | Posted: 7 June 2018 doi:10.20944/preprints201806.0126.v1

Peer-reviewed version available at Materials 2018, 11, 1147; doi:10.3390/ma11071147

concrete (strain capacity of ~0.01%), while the cost is much lower than ECC with oiled PVA fiber and PE fiber (strain capacity of 3−5%).

Selected microstructure analysis on the PP fiber and hydrophilic PVA fiber in matrix after the tensile test is presented in Figure 11. The SEM images show that the PP fiber has a smooth clear surface and a smooth cross-section, while the hydrophilic PVA fiber forms strong chemical bond with the matrix because the fiber surface is covered by hydrated products. The main failure model of hydrophilic PVA fiber is fracture, instead of pullout, which commonly occurred for oiled PVA.

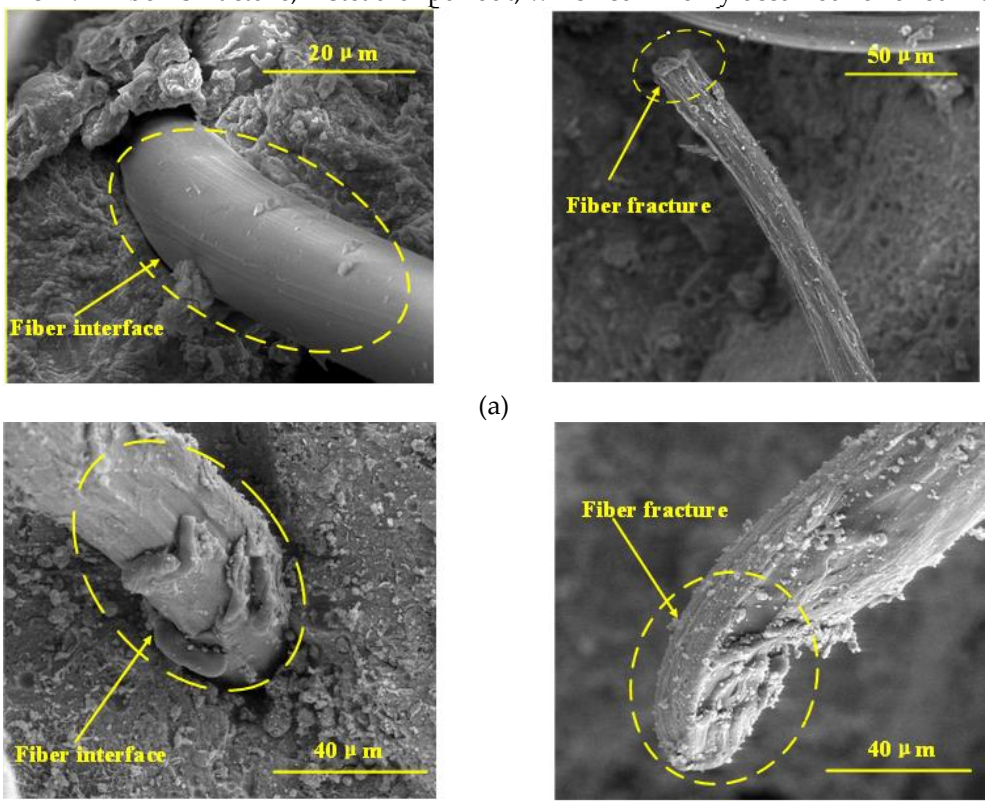

Figure 11. SEM photos: (a) PP fiber, and (b) Hydrophilic PVA fiber.

3.2. Durability ability

Carbonization test: Penetration of CO_2 in cementitious materials led to a reduction in pH and accelerated the corrosion of rebars, resulting in shorter useful life of constructions, which is a major concern in terms of practical applications [32]. In this study, the average carbonation depth was derived from Eq. (2).

$$\overline{d}_t = \frac{1}{n}\sum_{i=1}^{n} d_i \quad (2)$$

Figure 12 presents the carbonation depth of ECC specimens containing 2 vol% PP fiber. Carbonation depth depends on the porosity and pore size distribution of the hardened ECC matrix [33]. In ECC specimens, elimination of coarse aggregates and small amount of fine sands result in low porosity but high drying shrinkage of matrix. For example, the ultimate drying shrinkage of normal concrete is 400−600 μm/m [34], but conventional ECC can have 3 times that value under the same conditions. Some researchers have shown that PP fiber can reduce the depth of carbonation corrosion because of its cracking control ability [29]. As can be seen in Figure 13, the average corrosion depth is only 0.8 mm for a curing age of 28 days.

Preprints (www.preprints.org) | NOT PEER-REVIEWED | Posted: 7 June 2018 doi:10.20944/preprints201806.0126.v1

Peer-reviewed version available at Materials 2018, 11, 1147; doi:10.3390/ma11071147

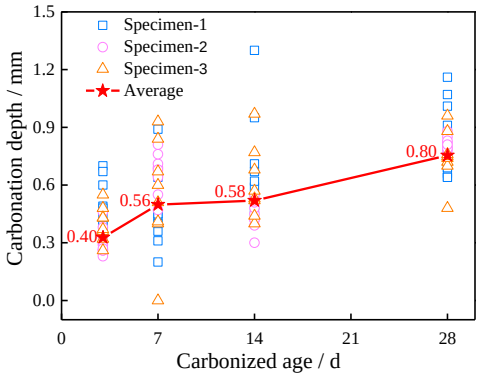

Figure 12. Carbonation depth of ECC specimens with 2 vol% PP fiber.

Carbonation corrosion test of rebar: Carbonation is one of the main factors leading to corrosion of reinforcement. Weight loss rate of rebar after corrosion under carbonation is determined herein. The influence on corroded rebar during pickling was also considered, and two plain rebars, named R01 and R02, were used as reference. The weight loss rate of rebar was derived according to Eq. (3), and the results are shown in Table 5.

$$L_w = \frac{\omega_0 - \omega - \frac{(\omega_{01} - \omega_1) + (\omega_{02} - \omega_2)}{2}}{\omega_0} \times 100 \quad (3)$$

where L_w is the weight loss rate of rebar (%); ω_0 and ω are the weights of the rebar before and after erosion of carbonation; for reference rebar, ω_{01} and ω_{02} are the initial weights, and ω_1 and ω_2 are the weights after pickling.

Table 5. Results of carbonization corrosion test of rebar for the ECC with 2 vol% PP fiber.

NO.	ω_0	ω	ω_{01}	ω_1	ω_{02}	ω_2	L_w(%)
R_{01}	-	-	55.516	55.142	-	-	-
R_{02}	-	-	-	-	57.046	56.733	-
R_1	49.085	48.711	-	-	-	-	0.062
R_2	52.276	51.887	-	-	-	-	0.087
R_3	55.691	55.312	-	-	-	-	0.064
R_4	57.737	53.345	-	-	-	-	7.012
R_5	50.668	50.289	-	-	-	-	0.070
R_6	58.949	58.587	-	-	-	-	0.031

As seen in Table 5, only 0.031−0.087% weight loss was obtained for rebar under carbonized corrosion. Figure 13 shows that corrosion occurred only when a combination of air, CO2, and water penetrated the weakness of the joints. Combined with the result of the carbonation test, which shows that PP-ECC has significant resistance to rebar carbonation, and that PP-ECC shows high carbonation durability.

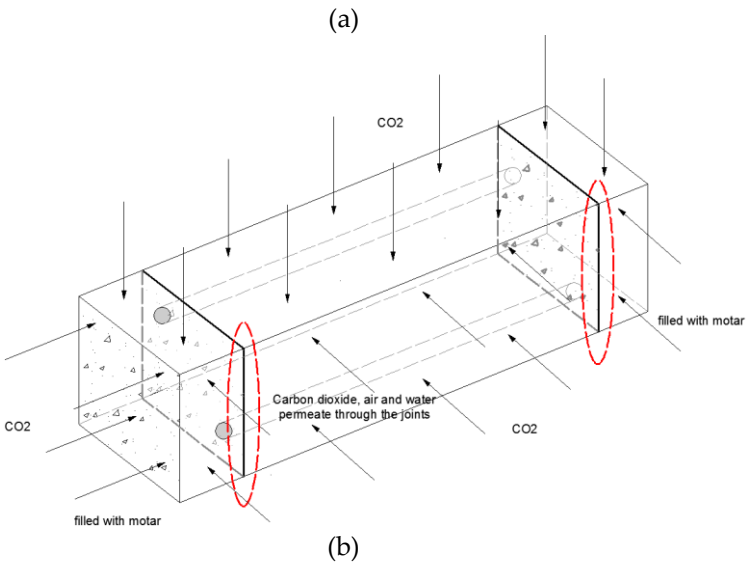

Figure 13. Carbonization corrosion tests of rebar for the ECC with 2 vol% PP fiber: (a) Corrosion parts, and (b) Erosion sketch.

4. Conclusion

This study investigated the mechanical properties and carbonation durability of ECC with various volume fractions of PP fibers and hydrophilic PVA fibers. Based on the above discussion, the following conclusion can be drawn:

1. Cost-efficient ECC materials can be obtained by addition of PP fibers, hydrophilic PVA fibers, and relatively coarse sand.
2. Compressive strength is increased upon increasing fiber content to 1 vol%, but decreased slightly beyond that volume fraction due to the dispersivity and air content created in the matrix by the higher volume fraction of the fiber.
3. Bending performance and impact resistance are both significantly affected by the fiber types and fiber contents. In general, cracking strength, post-cracking strength, and initial/final impact resistance energy increased with increasing fiber contents, and ECC materials with hydrophilic PVA fiber shows higher bending and impact resistance than those with PP fiber.
4. ECC materials with PP fiber and hydrophilic PVA fiber show lower strain capacity than those with oiled PVA fiber and PE fiber. However, low manufacturing cost make the ECC materials suitable for utilization.
5. Carbonation test on PP-ECC with 2 vol% PP fiber revealed a carbonation depth of only 0.8 mm, which illustrates superior carbonation durability and greater protection for rebar over prolonged use.

Author Contributions: The background research for this publication was carried out by all authors. Wei Zhang and Zhi-Yi Huang conceived and designed the experiments and wrote this manuscript. Wei Zhang, Cheng-Long Yin, and Fu-Quan Ma performed the experiments. All the authors participated in the analysis of experiments results.

Acknowledgments: This research was supported by the Zhejiang Provincial Important Research Project of China with Grant No. 2018C03029; and the Zhejiang Provincial Transportation Science and Technology Project of China with Grant No. 2018QNA4023.

Conflicts of Interest: The authors declare no conflict of interest.

Reference:

1. Herbert, E.N.; Li, V.C. Self-Healing of microcracks in engineered cementitious composites (ECC) under a natural environment. *Materials*. ***2013***, *6*, 2831-2845.

2. Khalil, A.E.H.; Etman, E.; Atta, A.; Essam, M. Behavior of RC beams strengthened with strain hardening cementitious composites (SHCC) subjected to monotonic and repeated loads. *Eng. Struct.* ***2017***, *140*, 151-163.
3. Yu, J.; Leung, C.K.Y. Strength Improvement of Strain-Hardening Cementitious Composites with Ultrahigh-Volume Fly Ash. *J. Mater. Civil. Eng.* ***2017***, *29(9)*, 05017003.
4. Georgiou, A.V.; Pantazopoulou, S.J. Behavior of Strain Hardening Cementitious Composites in Flexure/Shear. *J. Mater. Civil. Eng.* ***2017***, *29(10)*, 04017192.
5. Atta, A.M.; Khalil, A. Improving the Failure Mode of Over-Reinforced Concrete Beams Using Strain-Hardening Cementitious Composites. *J. Perform. Constr. Fac.* ***2016***, *30(5)*, 04016003.
6. Li, V.C.; MISHRA, D.K.; NAAMAN A.E.; Wight, J.K.; Lafave, J.M.; Wu, H.C.; Inada, Y. On the shear behavior of engineered cementitious composites. *Adv. Cem. Based Mater.* ***1994***, *1(3)*, 142-149.
7. MAALEJ, M.; LI, V.C. Flexural tensile-strength ratio in engineered cementitious composites. *J. Mater. Civ. Eng.* ***1994***, *6(4)*, 513-528.
8. Li, V.C.; LEUNG, C.K.Y. Steady-state and multiple cracking of short random fiber composites. *J. Eng. Mech.* ***1992***, *118(11)*, 2246-2264.
9. Kai, M.F.; Xiao, Y.; Shuai, X.L.; Ye, G. Compressive Behavior of Engineered Cementitious Composites under High Strain-Rate Loading. *J. Mater. Civ. Eng.* ***2017***, *29(4)*, 04016254.
10. Pakravan, H.R.; Jamshidi, M.; Latifi, M. Study on fiber hybridization effect of engineered cementitious composites with low- and high-modulus polymeric fibers. *Constr. Build. Mater.* ***2016***, *112*, 739-746.
11. Yu, K.Q.; Wang, Y.C.; Yu, J.T.; Xu, S.L. A strain-hardening cementitious composites with the tensile capacity up to 8%. *Constr. Build. Mater.* ***2017***, *137*, 410-419.
12. Liu, H.Z.; Zhang, Q.; Li, V.C.; Su, H.Z.; Gu, C.S. Durability study on engineered cementitious composites (ECC) under sulfate and chloride environment. *Constr. Build. Mater.* ***2017***, *133*, 171-181.
13. Xu, L.; Pan, J.L.; Chen, J.H. Mechanical Behavior of ECC and ECC/RC Composite Columns under Reversed Cyclic Loading. *J. Mater. Civ. Eng.* ***2017***, *29(9)*, 04017097.
14. Choi, M.S.; Kang, S.T.; Lee, B.Y.; Koh, K.T.; Ryu, G.S . Improvement in Predicting the Post-Cracking Tensile Behavior of Ultra-High Performance Cementitious Composites Based on Fiber Orientation Distribution. *Materials.* ***2017***, *10(1)*, doi:10.3390/ma9100829.
15. Gesoglu, M.; Guneyisi, E.; Muhyaddin, G.F.; Asaad, D.S. Strain hardening ultra-high performance fiber reinforced cementitious composites: Effect of fiber type and concentration. *Composites, Part B.* ***2016***, *103*, 74-83.
16. Meng, D.; Huang, H.; Zhang, Y.X.; Lee, C.K. Mechanical behaviour of a polyvinyl alcohol fibre reinforced engineered cementitious composite (PVA-ECC) using local ingredients. *Constr. Build. Mater.* ***2017***, *141*, 259-270.
17. Said, H.; Razak, H.A. The effect of synthetic polyethylene fiber on the strain hardening behavior of engineered cementitious composite (ECC). *Mater. Des.* ***2015***, *86*, 447-457.
18. Huan, Y.J.; Wei, W. J.; Jin, Y. Experimental Study on FRP-Reinforced PP ECC Beams Under Reverse Cyclic Loading. *Mech. Compos. Mater.* ***2014***, *50(4)*, 447-456.
19. Zhang, J.; Wang, Q.; Wang, Z.B. Properties of Polyvinyl Alcohol-Steel Hybrid Fiber-Reinforced Composite with High-Strength Cement Matrix. *J. Mater. Civ. Eng.* ***2017***, *29(7)*, 04017026.
20. Zhang, J.; Wang, Z.B.; Wang, Q.; Gao, Y. Simulation and test of flexural performance of polyvinyl alcohol-steel hybrid fiber reinforced cementitious composite. *J. Compos. Mater.* ***2016***, *50(30)*, 4291-4305.
21. Pakravan, H.R.; Latifi, M.; Jamshidi, M. Ductility improvement of cementitious composites reinforced with polyvinyl alcohol-polypropylene hybrid fibers. *J. Ind. Text.* ***2016***, *45(5)*, 637-651.
22. Sasmal, S.; Avinash, G. Investigations on mechanical performance of cementitious composites micro-engineered with poly vinyl alcohol fibers [J]. *Constr. Build. Mater.* ***2016***, *128*, 136-147.
23. Khan, M.I.; Fares, G.; Mourad, S. Optimized Fresh and Hardened Properties of Strain Hardening Cementitious Composites: Effect of Mineral Admixtures, Cementitious Composition, Size, and Type of Aggregates. *J. Mater. Civ. Eng.* ***2017***, *29(10)*, 04017178.
24. Tosun-Felekoglu, K.; Godek, E.; Keskinates, M.; Felekoglu, B. Utilization and selection of proper fly ash in cost effective green HTPP-ECC design. *J. Cleaner Prod.* ***2017***, *149*, 557-568.
25. Zhang, G.; Li, G.X. Effects of mineral admixtures and additional gypsum on the expansion performance of sulphoaluminate expansive agent at simulation of mass concrete environment. *Constr. Build. Mater.* ***2016***, *113*, 970-978.

26. Monosi, S.; Troli, R.; Favoni, O.; Tittarelli, F. Effect of SRA on the expansive behaviour of mortars based on sulphoaluminate agent. *Cem. Concr. Compos.* ***2011***, *33*, 485-489.
27. Yu, J.; Li, H.D.; Leung, C.K.Y.; Lin, X.Y.; Sham, I.M.L.; Shih, K. Matrix design for waterproof Engineered Cementitious Composites (ECCs). *Constr. Build. Mater.* ***2017***, *139*, 438-446.
28. Caggiano, A.; Gambarelli, S.; Martinelli, E.; Nistico, N; Pepe, M. Experimental characterization of the post-cracking response in Hybrid Steel/ Polypropylene Fiber-Reinforced Concrete. *Constr. Build. Mater.* ***2016***, *125*, 1035-1043.
29. Medina, N.F.; Barluenga, G.; Hernandez-Olivares, F. Combined effect of polypropylene fibers and silica fume to improve the durability of concrete with natural pozzolans blended cement. *Constr. Build. Mater.* ***2015***, *96*, 56-566.
30. Pan, Z.F.; Wu, C.; Liu, J.Z.; Wang, W.; Liu, J.W. Study on mechanical properties of cost-effective polyvinyl alcohol engineered cementitious composites (PVA-ECC). *Constr. Build. Mate.* ***2015***, *78*, 397-404.
31. El-Din, H.K.S.; Eisa, A.S.; Aziz, B.H.A.; Ibrahim, A. Mechanical performance of high strength concrete made from high volume of Metakaolin and hybrid fibers. *Constr. Build. Mate.* ***2017***, *140*, 203-209.
32. Martins, ROG.; Alvarenga, Rdss.; Pedroti, L.G.; de Oliveira, A.F.; Mendes, B.C.; de Azevedo, ARG. Assessment of the durability of grout submitted to accelerated carbonation test. *Constr. Build. Mate.* ***2018***, *159*, 261-268.
33. Turk, K.; Demirhan, S. Effect of limestone powder on the rheological, mechanical and durability properties of ECC. *Eur. J. Environ. Civ. En.* ***2017***, *21(9)*, 1151-1170.
34. Zhang, J.; Gao, Y.; Wang, Z.B. Evaluation of shrinkage induced cracking performance of low shrinkage engineered cementitious composite by ring tests. *Composites, Part B.* ***2013***, *52*, 21-29.